The solar wind and the Sun–Earth link

Plasma streams out from the Sun in the form of the solar wind. **Shadia Rifai Habbal** and **Richard Woo** examine the workings of this enigmatic link between the Earth and the Sun.

Abstract

The solar wind fills the space between the Sun and its planets, shapes the planetary environments and the heliosphere, and comes to a screeching halt at the heliopause, the boundary with the interstellar medium. This tenuous medium is a fertile environment for exotic plasma processes, most of which are not fully understood. It also holds the intimate secrets of the mechanisms heating the corona that continue to elude us. As the only accessible space plasma laboratory, we must continue its exploration in search of the processes that impact the Earth's environment and govern the evolution of stars and their planetary systems.

Hints of the existence of a flow of particles of solar origin, impinging on the Earth's magnetic environment, established by Gilbert in 1600, date back to observations of aurorae, sunspots, and cometary tails. While Gilbert also established the extension of the geomagnetic field into space, Graham (1724) discovered that this field could be perturbed, and Celsius (1741) discovered that the appearance of aurorae was accompanied by magnetic disturbances on the Earth's surface. On the other hand, de Mairan (1754) speculated the existence of an association between energetic particles from the Sun and the resulting geomagnetic disturbances. It was a century later that the first flare phenomenon was discovered by Carrington (1859) and Hodgson (1859), which was followed two days later by a great magnetic storm. Its assumed solar origin and timing implied speeds of at least 1000 km s^{-1}.

Almost another century passed before Chapman and Ferraro (1931) showed that electrically neutral streams of electrons and protons travelling at that speed would compress the sunwards side of the geomagnetic field, thus causing a geomagnetic storm. Observations made during total solar eclipses of spectral lines identified with highly ionized states of iron by Grotrian (1931), Lyot (1939) and Edlen (1942), led to the discovery of the million degrees corona. Consequently, Chapman (1954) pointed out that such a hot atmosphere was bound to extend to infinity as a result of the high electron conductivity. On the other hand, Biermann (1957) suggested that cometary tails were the result of an outflow of solar corpuscular radiation.

In 1958 Parker unified Chapman's view of a static corona and Biermann's suggestion of solar corpuscular radiation, to show that the two were consistent with a subsonic-supersonic outflow from the hot corona into interplanetary space, which he named the solar wind (for more details, see review by Parker 1999). The presence of cometary tails observed around the Sun at all heliographic latitudes and all phases of the solar cycle implied that the solar wind filled space.

Space probes and the solar wind

The first detection of a supersonic flow in interplanetary space was made by Gringauz *et al.* (1960), and the first direct measurements of speed, density and temperature were reported by Bonetti *et al.* (1963) with the Explorer 10 spacecraft as it meandered across the magnetopause. The unequivocal existence of the solar wind was established by the Venus Mariner 2 spacecraft, launched in 1962, when it became immersed in a continual flow once it crossed the Earth's magnetopause (Snyder and Neugebauer 1964). Spanning four months of continuous measurements, the flow was far from uniform. Over a time interval of a solar rotation, or approximately 27 days, the density varied from about 1 to 50 protons cm^{-3}, and the speed ranged from approximately 300 to 800 km s^{-1}. The highest speed coincided with the lowest density, and the anticorrelation between the two was consistent. Furthermore, the pattern of speed and density variation was found to recur a few times with the rate of the average 27 day solar rotation. This range in speeds corresponded to the predictions of Parker's isothermal solar wind model for a coronal temperature range of $1–2\times10^6$ K.

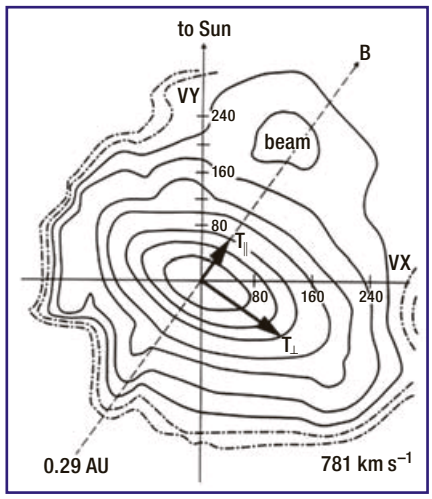

1: Proton velocity distribution functions measured in different solar wind streams by the spacecraft Helios. The straight dashed line gives the direction of the interplanetary magnetic field. The solar wind speed and distance to the Sun are indicated at the bottom; vectors indicate the temperature parallel and perpendicular to the magnetic field. (Adapted from Marsch 1991.)

Subsequent spacecraft measurements, with enhanced particle detection and ion composition techniques, led to the discovery of more intriguing properties. The solar wind was soon classified as either fast or slow, with the dividing line between the two attributed not only to speed but to composition, as well as to the different relative properties of the particles in these two types of streams. Measurements in the ecliptic plane established that the bulk of the solar wind consists of electrons and protons, and that alpha particles form the next most abundant ion (5% on average in fast streams), with traces of heavier ions being the same as detected spectroscopically in the photosphere. Electrons, protons and heavier elements do not have the same temperature. Furthermore, their temperature distribution is not isotropic, with the temperature parallel to the magnetic field direction being different from that in the perpendicular direction (figure 1). There is also evidence for differential flows, with heavier ions often flowing faster than the bulk electron–proton plasma in the fast streams. (For more details see reviews by Marsch 1991, 2003.)

The launch of the Ulysses spacecraft in 1990, with its flyby and gravity assistance by Jupiter in 1992, provided the first in-situ measurements

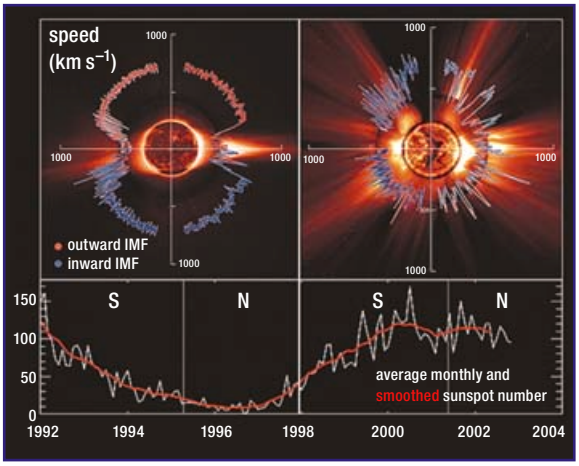

2: Polar plots of solar wind speed throughout the heliosphere as measured by Ulysses during the two polar orbits. The first one (left) coincided with the decline and minimum of solar activity. The second orbit (right) occurred during a period of enhanced and maximum solar activity. Also shown in each panel is a representative composite image of the corona in extreme ultraviolet (the disk image) and white light (off the limb), both from SOHO, from one day within each of these orbits. The lower panel shows the average monthly and smoothed sunspot number throughout the two orbits. (Courtesy D J McComas. See McComas *et al.* 2003.)

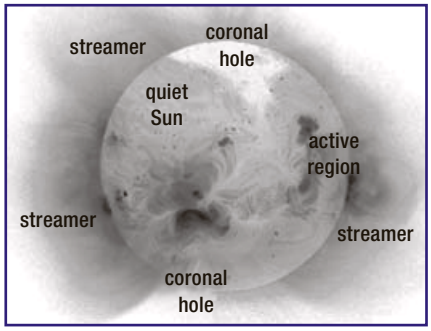

4: X-ray image of the corona taken with the Japanese spacecraft Yohkoh, with different regions identified with the terminology commonly used in solar physics.

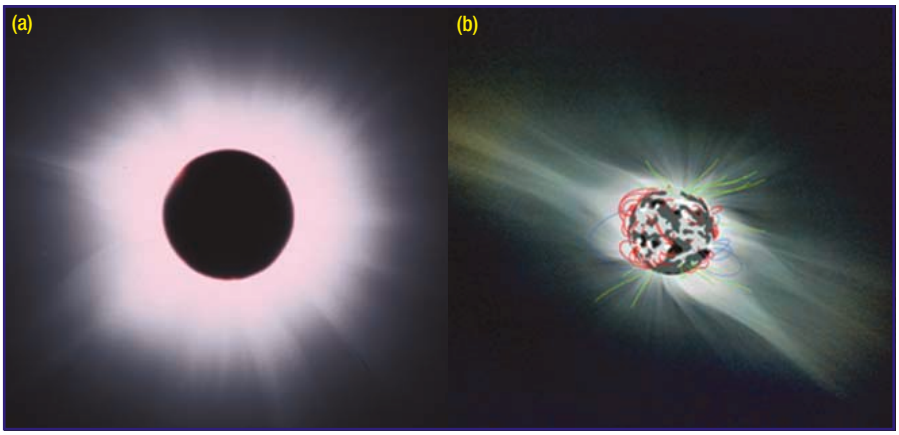

3: Eclipse images of the corona in white light on 11 August 1999 during solar maximum (a) and on 26 February 1998 during solar minimum (b). The thin coloured lines overlaid on the 1998 eclipse image are the results of source-surface magnetic field calculations, and trace the magnetic field lines resulting from these calculations. (Eclipse image courtesy Christian Viladrich, magnetic field line calculations courtesy Y-M Wang.)

of solar wind properties out of the ecliptic plane. While the signature of the solar wind in the heliosphere had already been determined from interplanetary scintillation of radio sources at different latitudes and as a function of solar cycle (e.g. Dennison and Hewish 1967, Coles *et al.* 1980, Kojima and Kakinuma 1987), the pole-to-pole measurements from Ulysses, having now spanned two solar cycles, confirmed that the variation of solar wind properties with latitude was solar-cycle dependent (figure 2). What emerged during the low activity part of the solar cycle was a fast wind dominating the heliosphere starting at ±20° above the ecliptic plane. In the region of ±20° about the ecliptic plane, the occurrence of fast and slow wind streams was the same as had been measured earlier by spacecraft bound to the ecliptic plane. As solar activity picked up, the interspersed fast and slow wind streams were no longer limited to low latitudes during the second pole to pole pass (figure 2).

Sources of the fast solar wind at the Sun

Given the magnetic nature of the Sun, and the close coupling between plasma and magnetic field, establishing the sources at the Sun of the solar wind flow is equivalent to identifying regions with a net outflow and open magnetic field lines, i.e. field lines rooted at the Sun but extending outwards with the flow into interplanetary space. To the naked eye, total solar eclipses reveal a filamentary, ever-expanding corona, stretching from the Sun into the infinity of space (figure 3a). Produced by the scattering of photospheric radiation by free electrons in the corona, this white light emission, which is thought to be a reflection of the coronal magnetic field, shows brighter features, known as helmet streamers, which extend the furthest away from the Sun, and are preferentially localized at low latitudes at solar minimum (figure 3b). At solar maximum (figure 3a), they appear indiscriminately at all latitudes.

With the advent of space exploration and spectroscopic imaging of the corona in the ultraviolet, extreme ultraviolet and X-rays, starting in the late 1960s, a "closed" corona dominated by arch-like structures associated with active regions emerged. Regions where X-ray emission was practically non-existent were dubbed "coronal holes", and the rest of the space where this emission was rather diffuse, was called "the quiet Sun" (figure 4). The cut-off in the radial extent of X-ray emission when compared to white light stems from the basic differences between white light and X-ray/EUV emission: namely a linear dependence on density in the former, versus a dependence on the square of the electron density and the electron temperature in the latter, thus leading to the dominance of the denser and hotter closed structures in X-ray emission.

The advent of simultaneous in-situ measurements in interplanetary space, and remote sensing observations of the corona in X-rays, led to the association of coronal holes with the source of the fast solar wind. The coincidence of in-the-ecliptic measurements of the longitudinal variation of solar wind speed exceeding 500 km s^{-1} with the passage at central meridian of the equatorwards extension of a polar coronal hole (figure 5), led Krieger *et al.* (1973) to conclude that coronal holes were the likely source of open magnetic field lines from which the fast solar wind originates. Extensions of the Parker transonic wind to the case of a dipolar solar magnetic field, compatible with white light images of the corona at solar minimum (e.g. Pneuman and Kopp 1971), also contributed to identifying polar coronal holes as the main source of the fast solar wind and of open magnetic field lines. Other approaches based on the extrapolation of the photospheric magnetic field using a potential field approximation and a fictitious source surface chosen around 2–2.5 $R_\odot$ as an outer boundary condition (e.g. Altschuler and Newkirk 1969), provided further support to this view when compared with white light images (as shown by the lines in figure 3b). These models identified streamers with the boundaries of coronal holes, and led to the concept of the superradial divergence of "open" magnetic field lines originating primarily from polar coronal holes. In the absence of coronal magnetic field or velocity measurements, such a view was readily adopted to account for the measured dominance of the fast solar wind in the heliosphere during the first Ulysses pole-to-pole pass.

However, given the preponderance of filamentary structures in the corona extending out into interplanetary space, as evidenced in eclipse white light images and radio occultation measurements (Woo 1996), one cannot help

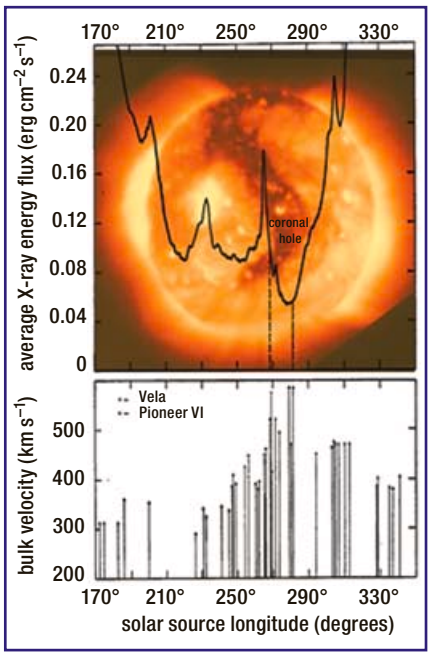

5: Plot of the average X-ray intensity of the corona at central meridian with the corresponding solar wind speed measurements in interplanetary space by Vela and Pioneer VI spacecraft. The background X-ray image is from Skylab and does not correspond to the same time period. It is merely shown to illustrate the central meridian passage of an equatorwards extension of a polar coronal hole causing a measurable dip in the X-ray intensity. (From Krieger *et al.* 1973.)

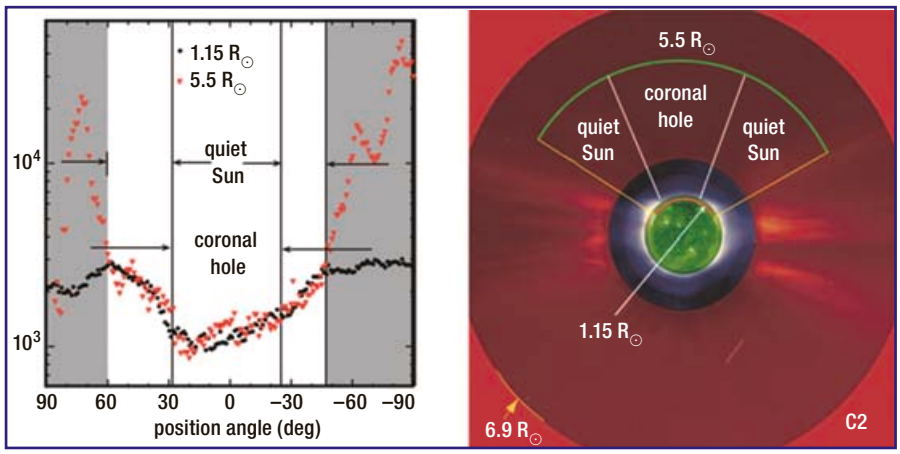

6: Plot of polarized brightness (or equivalently electron density) versus latitude at two different heights in the corona. The identification of the radial projection of the coronal hole and the quiet Sun is shown on the composite image in extreme ultraviolet and white light on the right. Position angle 0 corresponds to the north pole.

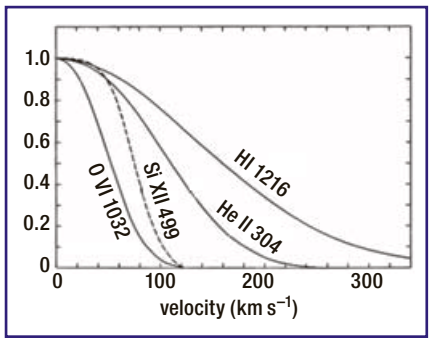

7: Plot of the calculated intensity of emission normalized to the corresponding intensity for ions at rest, versus outflow velocity, illustrating the effect of Doppler dimming. The calculations are for spectral lines formed in the ultraviolet and extreme ultraviolet. (From Withbroe *et al.* 1982.)

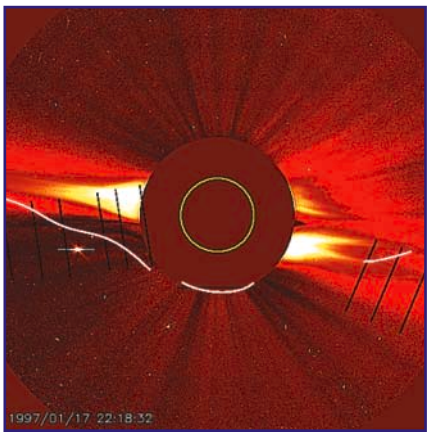

8: Constant velocity contour of 94 km s^{-1} inferred from the intensity ratio of 2 of the O VI 1032 and 1037 Å doublet measurements made with UVCS on 17 January 1997. The black lines give the different slit positions in the corona along which the measurements were made. The background is a white light image of the corona taken from LASCO/C2 on SOHO. (From Habbal *et al.* 1997.)

but question the rather simplifying view that the source of open field lines would be limited to coronal holes at the Sun. A different view of the source of the fast solar wind emerged first from investigations of the variation of the latitude of the electron density in the corona with radial distance (Woo and Habbal 1997). When observed off the limb close to the Sun, the contrast between coronal holes and their bounding regions is at most a factor of two in white light intensity, or equivalently density. Not only is this contrast preserved with radial distance, but so is the extent in latitude of the minimum of density as well as the relative difference in intensity between the radial extension of the coronal hole and its neighbouring regions (figure 6). This preservation of the latitudinal profile of density with heliocentric distance was interpreted by Woo and Habbal as evidence for a radial extension of the coronal plasma from both the coronal hole and the slightly higher density neighbouring quiet Sun.

That the preservation with radial distance of the latitudinal profile of electron density is also an indication of an outflow from coronal holes and the neighbouring quiet Sun, was further supported by the first inferences of solar wind speed in the inner corona, between 1.5 and 6 R$_\odot$. Based on the concept of resonance scattering of solar disk radiation by ions in the corona with the corresponding frequency of emission, these measurements became possible with the Ultraviolet Coronagraph Spectrometer (UVCS) on the Solar and Heliospheric Observatory (SOHO) launched in late 1995 (Kohl *et al.* 1997). Resonance scattering is maximum when the ions are at rest. However, once they start to drift with the solar wind flow, the condition of resonance at the rest frequency breaks down, and the resonant emission decreases in intensity, an effect known as "Doppler dimming" (Hyder and Lites 1970). By comparing the measured intensity with model calculations including outflows, a speed can be inferred (figure 7). Interestingly, the OVI doublet at 103.2 and 103.7 nm offers a convenient tool for a model-independent inference of 94 km s^{-1} for oxygen ions when the ratio of the line intensities equals 2 (Noci *et al.* 1987, Habbal *et al.* 1997). Using this diagnostic tool, a constant oxygen ion velocity contour of 94 km s^{-1} can thus be produced, as illustrated in the example of figure 8. The velocity contour of figure 8 indicates that there is an outflow in a significant fraction of the corona, not limited to the extension of the polar coronal hole.

By measuring the heliocentric distance along this contour (figure 9b), a proxy for the variation of velocity as a function of latitude at a given radial distance can be produced (Woo and Habbal 1999). Comparison of the variation with latitude of density and velocity shows that the two are anticorrelated in the corona (figure 9b). The pattern of variation of density and velocity as a function of latitude in the fast solar wind with speeds >600 km s^{-1}, measured by Ulysses during the first polar pass over the southern hemisphere, follows that measured in the inner corona (Habbal and Woo 2001) (figure 9a). In both coronal and interplanetary space measurements, the fast wind radially projected to the higher density quiet Sun is slower than the fast wind radially projected to the lower density polar coronal holes. Such a correspondence seems to imply that the fast wind originates from a significant fraction of the solar surface, encompassing the quiet Sun and not limited to polar coronal holes.

Another important result to emerge from the Ulysses measurements is the linear correlation between density and particle flux (i.e. the product of density and speed which is also a measure

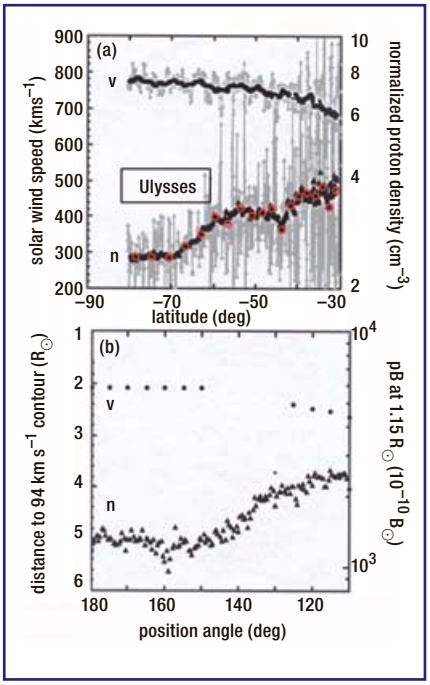

9: (a) Profiles of speed and density as a function of latitude during the south polar pass of the first orbit of Ulysses. Data points shown in grey are daily averages. The black points and triangles are 27-day sliding window averages. (b) Distance to the 94 km s^{-1} contour, used as a proxy for variation of speed with latitude in the corona, and density values derived from Mauna Loa polarized brightness measurements at 1.15 R$_\odot$ for the data of figure 8. (From Habbal and Woo 2001.)

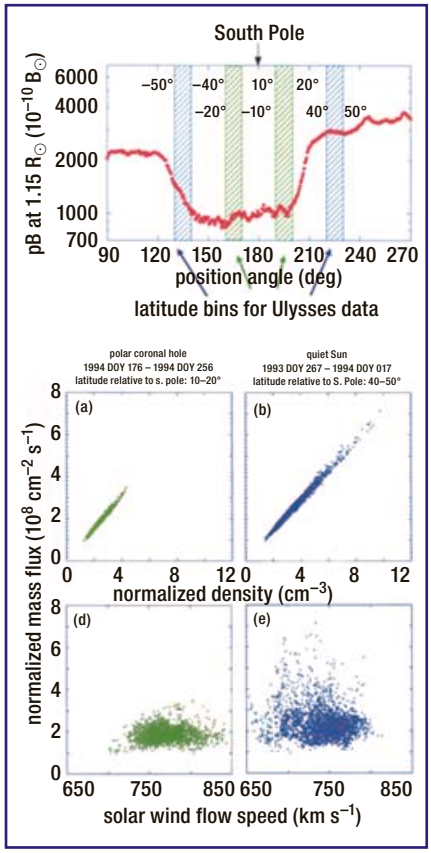

10: Variation of particle flux with density (a), (b) and velocity (d), (e) for the 10° latitude bins within a coronal hole (green) and the quiet Sun (blue). The data points in the top panel are produced from an average of the polarized brightness measurements at the Sun covering the time period of the corresponding Ulysses measurements in its first south polar pass. (Adapted from Habbal and Woo 2001.)

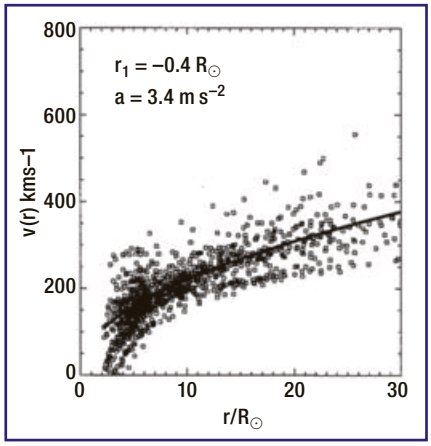

11: Solar wind velocity versus radial distance in a streamer calculated from time difference white light images. The solid curve is the root mean square best fit to the data points. (From figure 6 of Sheeley *et al.* 1997.)

of the solar wind mass loss rate). By separating the data in latitude bins radially projected to the latitudes within the polar coronal hole and the quiet Sun, it becomes evident that the range of densities and particle fluxes is a factor of two larger from the quiet Sun than from the coronal hole (figure 10).

The slow solar wind

Historically, the fast solar wind, with streams exceeding speeds of 500 km s^{-1} in interplanetary space, has been the focus of attention primarily because of the challenges facing the modelling of the physical processes capable of accounting for its observed properties. Yet the properties of the slow solar wind also offer valuable insight into the processes that control the coronal plasma. Radio occultation measurements in the inner corona yielded the first evidence of the slowest wind being associated with the tapering of the streamers into stalks (Woo and Martin 1997). Spectroscopic measurements with UVCS starting much closer to the Sun showed that the flow speed was negligible in the stalk out to 5 R$_\odot$ (Habbal *et al.* 1997, Strachan *et al.* 2002). Inferences of the speed in the slow solar wind from white light observations with the LASCO C2 and C3 coronagraphs on SOHO (Sheeley *et al.* 1997), yield a turbulent flow with speed profiles that match a Parker isothermal wind velocity profile of 1.2×10^6 K (figure 11); a curious result given the complex magnetic topology of streamers that are associated with the slow wind.

The role of closed magnetic structures in defining the distinguishing properties of the fast and slow wind was recently investigated by Woo *et al.* (2004). By considering composition measurements at the Sun and in the solar wind, together with the corresponding speed and density distributions, and the observational fact that elemental abundance enrichment at the Sun is associated with plasma confinement time (Feldman *et al.* 1998), these authors proposed that the trapping time is the distinguishing factor between fast and slow wind. The elemental abundance of plasma when trapped in closed magnetic structures – which abound at the base of the corona – for a long enough period of time, becomes enriched. The plasma is subsequently released into the solar wind by magnetic reconnection. However, the factors controlling the confinement time could not be identified in the data given the absence of coronal magnetic field measurements.

The elusive coronal magnetic field

The preponderance of filamentary density structures filling the corona and extending outwards from the Sun, and the ubiquitous detection of an outflow by spectroscopic measurements from UVCS throughout the corona beyond the 1.5 R$_\odot$ edge of the coronagraph, strongly suggest that the sources of the fast solar wind at the Sun cover a significant fraction of the solar surface. This is further supported by the preservation of the latitudinal variations of density and velocity with radial distance from the Sun into interplanetary space, as discussed above. Unfortunately, even with the highest spatial and temporal resolution photospheric magnetic field measurements, the fraction of the open magnetic flux that escapes from the Sun is unknown due to the paucity and difficulty of coronal magnetic field measurements.

The inference of the direction of the coronal magnetic field, through polarimetric imaging and spectroscopy of coronal forbidden lines, the strongest being in the near infrared, is the only tenable approach to establish the expansion of the coronal magnetic field from the photosphere outwards into interplanetary space. The first evidence that the coronal magnetic field expands almost radially from the solar surface appeared in the polarimetric images of the Fe XIII 1074.7 nm line by Eddy *et al.* (1973) during a total solar eclipse. Subsequent observations made with the coronagraph at Sacramento Peak Observatory yielded polarization maps spanning 1977–80, which also showed a predominant radial direction for the coronal magnetic field (Arnaud and Newkirk 1987). When placed in the context of contemporaneous white light images of the corona, the predominance of the radial direction of the magnetic field became even more striking as it stood in stark contrast with the "visually" nonradial aspect of the denser streamers (Habbal *et al.* 2001) (figure 12).

The dichotomy arising from recent observational evidences of the radial expansion of the

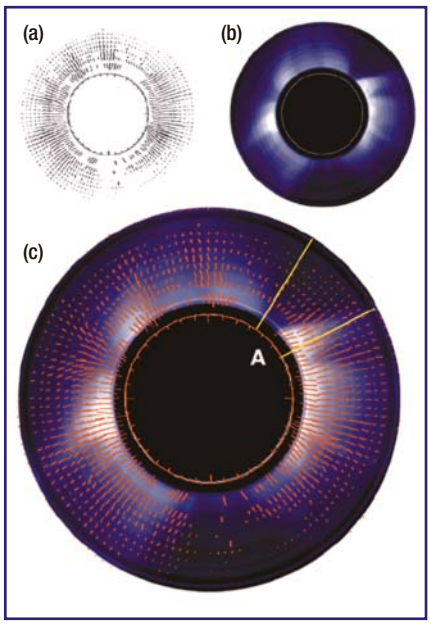

12: (a) Map of polarization angle of the Fe XIII 1074.7 nm emission from Sacramento Peak taken 23 February 1980. The orientation of the segments gives the direction of the magnetic field, while their lengths are proportional to the polarized intensity. Tick marks are position angles in increments of 10°. (b) Corresponding polarized brightness image from the Maua Loa K-coronameter. (c) An overlay of the two. The cone labelled A isolates a streamer and its vicinity, illustrating how there is no marked difference in polarization direction between the region coinciding with the streamer seen in white light and that directly adjacent to it. (From Habbal *et al.* 2001.)

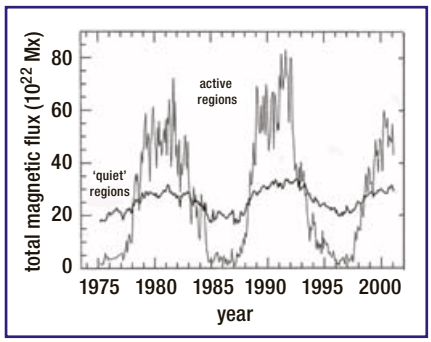

13: Variation of photospheric magnetic flux with time, covering almost three solar cycles. The separation between "active regions" and "quiet regions" was set at 25 G. (K L Harvey, private communication 2001.)

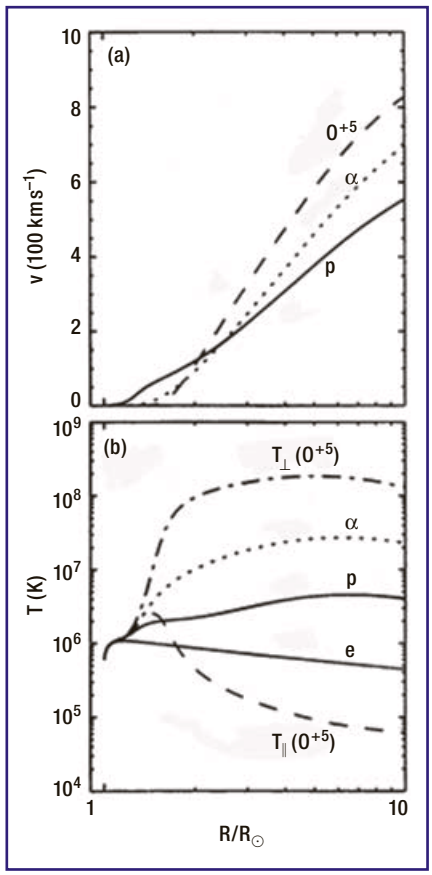

14: Speed and temperature for protons (p), oxygen ions (O^{+5}) and α particles from self-consistent multifluid model calculations invoking ion-cyclotron resonance. The choice of base parameters was such that the model calculations yielded the best match to observed values by UVCS. The results illustrate the occurrence of differential flows, and temperature anisotropies in the inner corona, in particular the fact that heavy ions flow faster than the bulk proton-electron solar wind. (From Li *et al.* 1998.)

solar wind is the coexistence of large-scale density structures in the corona, namely active regions, coronal holes and streamers, with the pervasive filamentary and almost radial density structures. In the absence of vector magnetic field measurements throughout the corona, this dichotomy will continue to exist. Hints at the possible existence of two sources for these distinct magnetic features are supported by recent model calculations of the solar dynamo (Cattaneo and Hughes 2001, further discussion by Bushby and Mason in this issue, page 4.7). These studies show that more than one dynamo could be operating in the solar interior, a deep one where the strong fields associated with active regions are rooted and undergo changes with the periodicity of the solar cycle or global field reversal, and a shallower dynamo likely to be the source of the pervasive small-scale field. Furthermore, the temporal distribution of different magnetic flux concentrations (< or >25 G) also shows a marked difference, with no solar-cycle dependence in the distribution of the weaker flux (figure 13). Support for the connection of the filamentary density structures to the solar interior are also present in observations of correlations between the latitudinal dependence of the statistical characteristics of the coronal polarized brightness, the subsurface differential rotation inferred from helioseismology, and Ulysses solar wind density measurements (Woo *et al.* 2000).

Waves in the solar wind

The acceleration of the solar wind cannot be dissociated from the heating of the corona (which is discussed elsewhere in this issue, page 4.34–4.37). The properties of the fast solar wind pose the more challenging constraints, with a rapid acceleration in the inner corona reaching the interplanetary asymptotic speed, exceeding 700 km s^{-1}, by 10 R$_\odot$, as inferred from radio scintillation measurements (Grall *et al.* 1995) and UVCS spectral line measurements (Li *et al.* 1998, Cranmer *et al.* 1999).

Investigations of the coronal sources of energy and momentum have been blessed and complicated by the distinct properties of electrons, protons and trace heavier elements in the solar wind. Interplanetary space measurements were the first to show that heavier ions move faster than protons in fast streams (Marsch 1991). Such properties were subsequently discovered in the inner corona with models attempting to account for the spectroscopic measurements by UVCS/SOHO (Li *et al.* 1998) (figure 14). In both interplanetary and coronal measurements, the temperature of heavier ions is found to be more than mass-proportional. While in-situ measurements yield temperature anisotropies in the core of the velocity distributions of protons in fast streams, but more Maxwellian-like distributions in slow streams (figure 1), spectroscopic measurements show evidence for broader than expected spectral lines of protons and heavy ions in the inner corona.

The search for the elusive physical processes was strongly influenced by the discovery of signatures of Alfvén waves in the solar wind (Belcher and Davis 1971). Models based on low-frequency Alfvén waves, as observed in interplanetary space, are relatively successful in accounting for the acceleration of the solar wind in the corona, but are not a direct source of heat for the wind. A paradigm for coronal heating, proposed in the late 1980s, was the ion-cyclotron resonance of high-frequency Alfvén waves generated by the turbulent cascade of low-frequency Alfvén waves (Hollweg 1986, 2003). However, the source of the waves remains unknown. Inferences from spectral line widths yield the needed wave pressure, but information regarding the frequency of these waves remains very scant. Recent measurements in active regions (Ulrich 1996) point to the likely existence of Alfvén waves with periods of 5 minutes. Measurements in the corona point to compressive waves with periods of 5–10 minutes (Morgan *et al.* 2004). However, conditions for ion-cyclotron resonance require high-frequency waves. At present, the turbulent cascade from low to higher frequency Alfvén waves, postulated in models, has yet to be established observationally. While the process of ion-cyclotron resonance has been successful in accounting for the main properties of protons and heavier ions in the solar wind (e.g. Li *et al.* 1999), the heating of the electrons remains problematic. Models yield electron temperatures that are too low in the fast solar

wind when compared to coronal values inferred from spectral line observations and from charge state measurements.

In addition to their role in accelerating the fast solar wind, Grappin *et al.* (2002) recently showed how Alfvén waves can also change the 2-D coupled magnetic and hydrodynamic geometry of the solar wind and its global stability, as well as the structure of both open and closed magnetic structures in the corona. Such a study illustrates that Alfvén waves might, in some cases, play a role in shaping the corona and the solar wind.

Aurorae: signs of the Sun–Earth link

Exploration of the solar wind phenomenon extends beyond that of a rich space plasma laboratory as its impact on the Earth's magnetic environment emerged with its discovery. Almost three centuries ago, aurorae were identified with geomagnetic disturbances and were associated with solar activity. The solar flare event of 1859 detected by Carrington and Hodginson, which was the first flare to be observed in white light, was followed a few days later by a significant geomagnetic disturbance. Observations of the recurrence of geomagnetic disturbances with the approximate 27-day solar rotation period, lent further support for their connection with particle streams originating from a fixed source at the Sun, which were named M-regions by Bartels (1932). The association of geomagnetic disturbances with energetic particles escaping from active regions was further supported by the period between 1620 and 1716, known as the Maunder Minimum, when a very low number of recorded sunspots coincided with very few aurorae seen in Europe during that time period. With the advent of solar wind measurements in the late 1960s and early 70s, enhanced geomagnetic disturbances were soon observed to be associated with exceptionally fast solar wind streams. And, when coronal mass ejections were first discovered in space-borne white light coronagraph images, as huge bubble-shaped and/or twisted structures, expanding outwards from the Sun, they were subsequently found to trigger enhanced geomagnetic disturbances when Earth-directed. Does our understanding of geomagnetic disturbances then merely follow the latest phenomenon discovered in interplanetary space, or is it that virtually all sudden changes in the solar wind can lead to geomagnetic disturbances?

Just as the solar wind is a consequence of fundamental physical laws, so is the Earth's magnetic environment. It is the interaction of the magnetized solar wind plasma with the Earth's static field that creates the asymmetric magnetosphere, a distorted dipole compressed in the sunward direction as a consequence of the solar wind dynamic pressure impinging upon this stationary obstacle (Chapman and Ferraro 1931). Another fundamental plasma property proposed by Dungey (1961), which accounts for the shape of the stretched magnetosphere in the anti-sunwards direction by the solar wind flow, is magnetic reconnection. When oppositely directed magnetic fields are pressed together, there develops a (relatively) small region in space where the magnetic field lines are no longer tied to the ionized gas as a consequence of its infinite conductivity. Rather, the fields are able to diffuse and "reconnect", thereby not only changing their original topologies, but also enabling the exchange of charged particles originally associated with the two parent fields. As the Earth's magnetic field, in its latest reversal is northwards pointing, magnetic reconnection is favoured when the interplanetary solar magnetic field, or IMF, is southwards pointing. The combination of solar wind dynamic pressure and magnetic reconnection leads to the formation of the tear-drop shaped magnetosphere, and the entry of solar energetic particles into the Earth's ionosphere. Such a scenario can exist in a somewhat steady state. However, any change in either reconnection or solar wind dynamic pressure will cause disturbances in the geomagnetic field as a result of induced currents. By considering these fundamental plasma processes, it then becomes clear that flares, coronal mass ejections or fast solar wind streams, which can all lead to sudden changes in solar wind dynamic pressure, can trigger geomagnetic storms. The strength of the storm, and the latitudes at which it can be detected, is then directly related to the magnitude of the resulting disturbance of the geomagnetic field.

Conclusions

As space exploration continues to expand by building upon new discoveries, the solar wind seems to hold on to the tantalizing secrets not only of the hot corona, but the solar interior as well. By pushing the limits of technology to try to reach closer to the Sun, chances of achieving breakthroughs in our understanding of some of the fundamental physical processes that control the Sun and its environment should be enhanced. Missions such as Solar Orbiter, which will image the Sun above the ecliptic plane, and will be orbiting the Sun synchronously at some periods of time, or the proposed Solar Probe that will be the first spacecraft to enter the solar corona and directly probe it in its pole-to-pole trajectory around the Sun, are bound to unravel more secrets. By coupling these measurements with ground-based polarimetric spectroscopy (Lin *et al.* 2000), which is forging the way for exploring the most fundamental plasma property, namely the coronal magnetic field, access to the most direct link between the solar interior, the corona and the interplanetary space should become tenable. ●

Prof. Shadia Rifia Habbal, Dept of Physics, University of Wales, Aberystwyth. Dr Richard Woo, Jet Propulsion Lab, Pasadena, Califiornia, USA. *The authors are grateful to R Grappin for a constructive review.*

References

Altschuler M D and Newkirk G 1969 *Solar Phys* **9** 131.
Arnaud J and Newkirk G A Jr 1987 *A&AS* **178** 263.
Bartels J 1932 *Terrest Magn Atmos Elect* **37** 1.
Belcher J W and Davis L Jr 1971 *J Geophys Res* **76** 3534.
Biermann L 1957 *Observatory* **77** 109.
Bonetti A *et al.* 1963 *J Geophys Res* **68** 4017.
Carrington R C 1859 *MNRAS* **20** 13.
Cattaneo F and Hughes D W 2001 *A&G* **42** 3.18–3.22.
Celsius A 1741 *Svensk Vel Acad Handl* **1** 391.
Chapman S 1954 *ApJ* **120** 151.
Chapman S and Ferraro V C A 1931 *Terrest Magn Atmos Elec* **36** 77.
Coles *et al.* 1980 *Nature* **286** 239–41.
Cranmer S R *et al.* 1999 *ApJ* **511** 481.
De Mairan J J dOr 1754 *Suite de Mem Acad Roy Sci*, Paris, 2nd edition.
Dennison P A and Hewish A 1967 *Nature* **28** 343–46.
Dungey J W 1961 *Phys Rev Lett* **6** 47–48.
Eddy J A *et al.* 1973 *Sol Phys* **30** 351.
Edlen B 1942 *Z Astrophys* **22** 30.
Gilbert W 1600 *De Magnete*, London (in Latin), translated by P F Mottelay, Dover Publications, New York 1958.
Graham G 1724 *Phil Trans Roy Soc London* **A 32** 96.
Grall R R *et al.* 1995 *Nature* **379** 429.
Grappin R, Leorat J and Habbal S R 2002 *J Geophys Res* **107** doi:10.1029/2001JA005062, SSH 16-1.
Gringauz K I *et al.* 1960 *Soviet Phys Doklady* **5** 361.
Grotrian W 1931 *Z Astrophys* **3** 199.
Habbal S R *et al.* 1997 *ApJ* **489** L103.
Habbal S R and Woo R 2001 *ApJ* **549** L253.
Habbal S R *et al.* 2001 *ApJ* **558** 852.
Hodgson R 1859 *MNRAS* **20** 15.
Hollweg J V 1986 *J Geophys Res* **91** 4111.
Hollweg J V 2003 in *Solar Wind Ten* eds M Velli, R Bruno and F Malara, AIP CP679, New York,14–20.
Hyder C L and Lites B W 1970 *Solar Phys* **14** 147.
Kohl J L *et al.* 1997 *Solar Phys* **175** 613.
Kojima M and Kakinuma T 1987 *J Geophys Res* **92** 7269.
Krieger A S *et al.* 1973 *Solar Phys* **23** 123.
Li X *et al.* 1999 *J Geophy. Res* **104** 2521.
Li X *et al.* 1998 *ApJ* **501** L133.
Li X and Habbal SR 2003 *ApJ* **598** L125–L128.
Lin H *et al.* 2000 *ApJ* **541** 83.
Lyot B 1939 *MNRAS* **99** 580.
Marsch E 1991 in *Physics of the Inner Heliosphere* eds R Schwenn and E Marsch, Springer-Verlag, Heidelberg, **vol II** 45.
Marsch E 2003 in *Solar Wind Ten* eds M Velli, R Bruno and F Malara, AIP CP679, New York, 399–404.
McComas D J *et al.* 2002 *Geophys Res Lett* **30** doi 10.1029/2003GL017136.
Morgan H *et al.* 2004 *ApJ* **605** 521–27.
Neugebauer M and Snyder CW 1966 *J Geophys Res* **71** 4469.
Noci G *et al.* 1987 *ApJ* **315** 706.
Parker E N 1958 *ApJ* **128** 664.
Parker E N 1999 in *Solar Wind Nine* eds S R Habbal, R Esser, J V Hollweg and P A Isenberg, AIP CP471, New York, 3–13.
Pneuman G W and Kopp R A 1971 *Solar Phys* **18** 258.
Sheeley N R Jr *et al.* 1997 *ApJ* **484** 472.
Snyder C W and Neugebauer M 1964 *Space Res* **4** 89.
Strachan L *et al.* 2002 *ApJ* **571** 1008.
Ulrich R 1996 *ApJ* **465** 436.
Withbroe G L *et al.* 1982 *Space Sci Rev* **33** 17–52.
Woo R 1996 *Nature* **379** 321.
Woo R and Habbal S R 1997 *Geophys Res Lett* **24** 97.
Woo R and Habbal S R 1999 *Geophys Res Lett* **26** 1793.
Woo R and Martin J 1997 *Geophys Res Lett* **24** 2535.
Woo R *et al.* 2000 *ApJ* **538** L171.
Woo R, Habbal S R and Feldman U 2004 *ApJ* in press.